

- (12) (a) Chien, J. C. W.; Karasz, F. E.; Wnek, G. E.; MacDiarmid, A. C.; Heeger, A. J. *J. Polym. Sci., Polym. Lett. Ed.* **1979**, *18*, 45. (b) Bernier, P.; Rolland, M.; Linays, C.; Disi, M. *Polymer* **1980**, *21*, 7.
- (13) Chien, J. C. W.; Yang, X. *J. Polym. Sci., Polym. Lett. Ed.* **1983**, *21*, 767.
- (14) Epstein, A. J.; Rommelmann, H.; Druy, M. A.; Heeger, A. J.; MacDiarmid, A. G. *Solid State Commun.* **1981**, *38*, 683.
- (15) Weinberger, B. R.; Kaufer, J.; Heeger, A. J.; Pron, A.; MacDiarmid, A. G. *Phys. Rev. B: Condens. Matter* **1979**, *20*, 223.
- (16) Campbell, D. K.; Bishop, A. R. *Phys. Rev. B: Condens. Matter* **1981**, *24*, 4859. (b) Bredas, J. L.; Chance, R. R.; Silbey, R. *Phys. Rev. B: Condens. Matter* **1982**, *26*, 5843 (1982).
- (17) (a) Kivelson, S. *Phys. Rev. Lett.* **1981**, *46*, 1344. (b) Kivelson, S. *Phys. Rev. B: Condens. Matter* **1982**, *25*, 3798.
- (18) (a) Ikehata, S.; Kaufer, J.; Woerner, T.; Pron, A.; Druy, M. A.; Sivak, A.; Heeger, A. J.; MacDiarmid, A. G. *Phys. Rev. Lett.* **1980**, *45*, 1123. (b) Epstein, A. J.; Rommelmann, H.; Druy, M. A.; Heeger, A. J.; MacDiarmid, A. G. *Solid State Commun.* **1981**, *38*, 683.
- (19) (a) Su, W. P.; Schrieffer, J. R. *Proc. Natl. Acad. Sci. U. S. A.* **1980**, *77*, 5626. (b) Bryant, G. W.; Glick, A. J. *Phys. Rev. B: Condens. Matter* **1982**, *26*, 5855.
- (20) Chien, J. C. W.; Babu, G. N. *J. Chem. Phys.* **1985**, *82*, 441.

## Polarized Raman Measurements of Structural Anisotropy in Uniaxially Oriented Poly(vinylidene fluoride) (Form I)

Laurie Lauchlan and John F. Rabolt\*

IBM Almaden Research Center, San Jose, California 95120. Received March 26, 1985

**ABSTRACT:** The anisotropic scattering properties of a uniaxially oriented filament of planar zigzag (form I) poly(vinylidene fluoride) have been investigated by polarized Raman scattering measurements. Results indicate that the assignment of the observed bands to specific symmetry species is straightforward and suggest that IR and Raman bands previously assigned from studies on drawn films should be reexamined. Comparison of these new assignments with those calculated from existing valence force fields gives a reasonable agreement but suggests that the force field could be improved by refinement incorporating these latest results. In addition, the observation of a low-frequency Raman active longitudinal acoustical mode and the correlation of its frequency with the crystalline stem length obtained from small-angle X-ray scattering and crystallinity measurements are shown to reflect the trans planar conformation of form I.

### Introduction

Considerable interest in poly(vinylidene fluoride) (PVF<sub>2</sub>) continues to exist because of the piezo- and pyroelectric properties that are exhibited by certain of its crystalline forms.<sup>1-3</sup> Recently it has also been shown that random copolymers of vinylidene fluoride and trifluoroethylene exhibit ferroelectric behavior over a specific range of comonomer concentration,<sup>4</sup> again leading to a flourish of research activity<sup>5,6</sup> designed to understand the mechanism responsible for this effect.

Although vibrational spectroscopy, in general, has played only a minor role in unraveling the physics of piezoelectricity in polymers, it has played a more important role in identifying the conformational structure of the molecular backbone responsible for piezoelectric behavior. Infrared studies<sup>7-11</sup> have been reported on all three crystalline forms of PVF<sub>2</sub> with band assignments being made from polarized measurements obtained from oriented films. In most cases agreement between the observed bands and those determined from normal coordinate calculations has been satisfactory,<sup>10,11</sup> but a complete set of assignments has not been available.

On the other hand Raman studies<sup>12</sup> on oriented films have been much more complicated due to the relatively small thickness of films after orientation (hence a small scattering volume) and, perhaps more seriously, polarization scrambling of the incident and scattered light due to domains in the film that reduce its transparency in the visible. This latter problem is a general one in polymers and, as such, has prevented Raman polarization studies in all but the simplest cases. The potential of such studies is great since, together with a group theoretical analysis, it provides a means of identifying the symmetry of the observed bands, information that can then be used to refine existing force fields.<sup>10,11</sup> Another important utility

of polarized Raman measurements is to differentiate between proposed conformational structures since, in many cases, alternate structures dictate a different set of spectroscopic selection rules from which a comparison with experimental observations can be made.

Our own studies<sup>13</sup> of anisotropic Raman scattering in uniaxially oriented polymers have progressed over the past several years because of the availability of transparent highly oriented monofilaments that have found use in high-modulus applications. Recently, in Raman studies on an alternating copolymer of ethylene and tetrafluoroethylene (E-TFE)<sup>13</sup> it was determined that the conformational structure was, in fact, planar zigzag, not helical, a subject of some controversy in the past.<sup>14,15</sup> In order to draw that conclusion from polarized Raman measurements, a group theoretical formalism was derived<sup>16</sup> to predict spectroscopic activity for polymers whose main axis of symmetry is perpendicular to the direction of uniaxial orientation. These expressions are generally applicable to all planar zigzag structures and thus have been applied to a study of PVF<sub>2</sub> (form I) in this current work. In conjunction with this analysis the anisotropic scattering properties of a highly oriented uniaxial filament were measured in a number of sample geometries, allowing specific band assignments to be made. A set of revised band assignments is proposed and reasons for discrepancies with previous work are discussed.

### Experimental Section

The PVF<sub>2</sub> sample used in this study was provided as a 0.01-in. diameter filament by Albany Monofilament Co. It was produced by extrusion through a pinhole die followed by a ~4× draw. The source of the PVF<sub>2</sub> polymer was Pennwalt Corp., and, as such, this material contained 5-6% head-head defects.

Polarized Raman measurements were obtained with a Jobin-Yvon HG-2S double monochromator equipped with an RCA

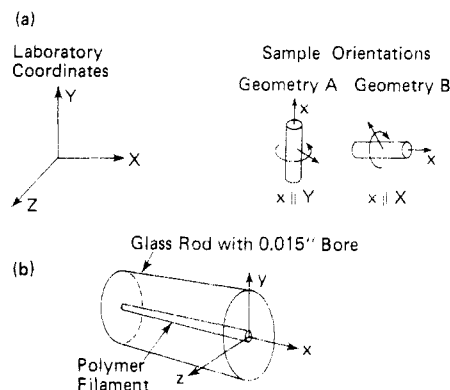


**Figure 1.** (a) Schematic diagram of the two different scattering geometries used for polarized Raman measurements:  $XYZ$ , laboratory axes;  $xyz$ , molecular axes. (b) Experimental arrangement used in scattering geometry B.

31034A-02 photomultiplier tube and standard photon-counting electronics. Digital data were recorded with a Nicolet 1180 data system, which was used to co-add multiple scans. The source of excitation was provided by a Spectra Physics 165-08 argon ion laser operating at 488.0 nm with 250 mW of power incident on the sample. Prior to impinging on the monofilament, the incident beam was passed through a Glan-Thompson prism to ensure the selection of only one polarization component. The Raman scattered light was passed through an analyzer ( $\sim 99\%$  efficiency) that could be aligned either parallel or perpendicular to the entrance slit of the double monochromator. Because of the anisotropic diffraction properties of holographic gratings, a polarization scrambler was placed between the analyzer and the entrance slit. Rotation of the polarization of the incident beam by  $90^\circ$  coupled with the two orthogonal positions of the analyzer ( $Y$  and  $X$  in Figure 1) provided four independent polarized Raman measurements for a given sample geometry.

Very low-frequency Raman measurements were obtained by placing an iodine vapor cell between the collection lens and the entrance slit of the monochromator.<sup>17</sup> By placing an etalon in the cavity of the argon ion laser, only one of the 60 or more resonant modes that fall under the 514.5-nm Doppler gain curve can be selected. Adjustment of the etalon so as to choose a mode<sup>17</sup> that corresponds exactly to the difference between two rotational energy levels of  $I_2$  can then be made. Then when the scattered light is collected and passed through this molecular filter, the Rayleigh (elastic) scattered component is attenuated by 3–6 orders of magnitude while the Raman (inelastic) scattered component is reduced by 50%, allowing spectra to be recorded within  $3\text{ cm}^{-1}$  of the exciting line.

The conventional scattering geometry for recording the Raman spectrum of a monofilament is illustrated in Figure 1a using geometry A. However, in order to unequivocally identify the symmetry species of each band, a second scattering geometry (B) was also used as shown in Figure 1b. In this case, a PVF<sub>2</sub> filament (0.01-in. diameter) that had been cut with a sharp blade was placed inside the bore (0.015-in. diameter) of a glass rod. With this method, the tightly focused incident beam (using a 50-mm achromat lens) could be brought through the end of the filament. Scattered light from the first 2–3 mm was collected at  $90^\circ$  through the glass and focused on the entrance slit of the double monochromator with an  $f/1.8$  Berthiot lens. When the collection of scattered light was restricted to the entrance end of the filament, polarization scrambling was minimized.

## Results and Discussion

**Identification of Crystalline Modification.** In order to estimate the extent of orientation as well as the presence of any other crystalline modifications in the monofilament a number of characterization experiments were undertaken. A wide-angle X-ray diffraction (WAXD) photograph revealed that the sample contained primarily highly ordered form I crystals as evidenced by the appearance of a highly arced diffraction pattern similar to that observed by McGrath and Ward<sup>18</sup> for PVF<sub>2</sub> drawn 5 times at  $T =$

$80^\circ\text{C}$ . A small amount of residual form II was still present and was estimated<sup>18</sup> to be less than 10% by volume.

Small-angle X-ray scattering (SAXS) measurements of the PVF<sub>2</sub> filament yielded a four-point pattern indicative of highly oriented lamellae whose surface normals are tilted at an angle of  $24\text{--}26^\circ$  with respect to the filament axis. Polarized measurements of the Raman-active longitudinal acoustical mode (LAM) indicated that, within experimental error, the chain stems are parallel to the filament axis and hence inclined at an angle of  $64\text{--}66^\circ$  with respect to the lamella surface. The observed long period for the filament used in this study was  $103\text{ \AA}$ .

In order to quantify the presence of other crystalline modifications, far infrared measurements were undertaken in the  $20\text{--}110\text{-cm}^{-1}$  region, where lattice vibrations characteristic of the different crystalline modifications have been observed. Rabolt and Johnson<sup>9</sup> and Kobayashi et al.<sup>10</sup> have shown that the presence of form II crystals are manifested by a medium band at  $52\text{ cm}^{-1}$  that involved intermolecular vibration of the two chains in the unit cell. If, on the other hand, form I or form III is present, broad strong bands at  $70$  and  $100\text{ cm}^{-1}$  are observed, respectively.<sup>10</sup>

In order to obtain the far infrared spectrum of the filament, a number of small pieces were cut, placed parallel to one another, and subjected to high pressure in order to essentially "flatten" the sample. Several of these were fixed to a metal washer and run in a transmission mode. In addition a small piece was also investigated by Raman scattering to ensure that the high compression did not result in a phase transformation. Results indicated that no change had occurred while the IR measurements revealed the presence of a broad band at  $74\text{ cm}^{-1}$ . No evidence of a band at  $52\text{ cm}^{-1}$  characteristic of form II was found, although at the low concentrations suggested by WAXD it could easily be obscured by the breadth and intensity of the  $74\text{-cm}^{-1}$  band.

Thus the WAXD and IR measurements confirmed that the specimen used in this study contained predominantly highly oriented form I crystals.

**Raman Measurements.** Although Raman studies of PVF<sub>2</sub> (form I) have appeared in the past,<sup>12,19</sup> a satisfactory assignment of the observed bands has not occurred because of poorly oriented samples. Snyder<sup>20</sup> has derived the expressions for the Raman scattering activities in terms of the principal axes of polarizability of the molecule for the case where the symmetry axis of the polymer chain was parallel to the orientation axis in a uniaxially oriented system. Although this analysis is useful in partially oriented systems where the conformation of the backbone is helical and the symmetry axis is along the molecular axis, there are a number of cases with conformations that cannot be analyzed with these expressions. In these cases, the symmetry axis is perpendicular to the direction of uniaxial orientation and an alternative<sup>16</sup> symmetry analysis is required. Early work<sup>19</sup> proposed a general method of permutation of the  $x$  and  $z$  axes in Snyder's expressions to obtain a new set of expressions applicable to cases where the symmetry axis is perpendicular to the orientation direction. This treatment, in general, is not valid for most point-group symmetries but does fortuitously give the correct symmetry assignments for planar zigzag PVF<sub>2</sub> ( $C_{2v}$  point group).

Satisfactory classification of all bands to their respective symmetry species often requires different sampling geometries as illustrated in Figure 1a. In geometry A the  $x$  axis of the sample is parallel to the laboratory fixed coordinate,  $Y$ , while in geometry B it is parallel to  $X$ . As alluded to

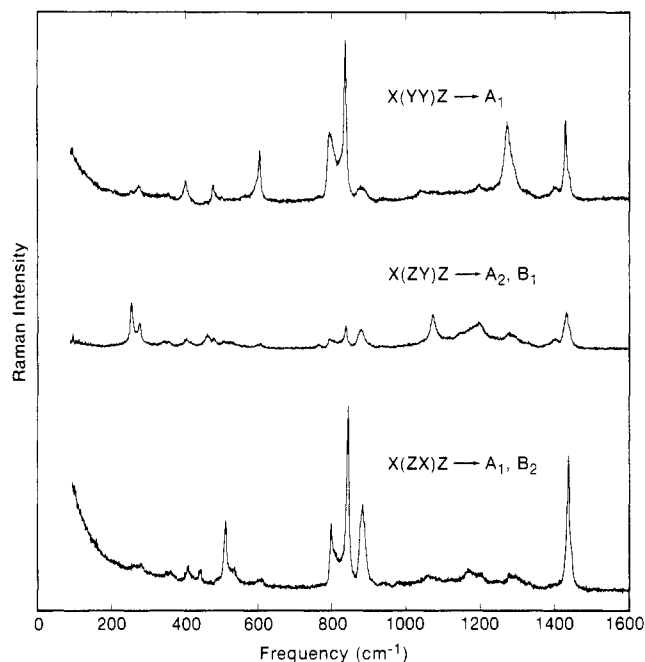


**Figure 2.** Polarized Raman measurements obtained with geometry A with the laser incident along *X* and the scattered radiation collected along *Z*. The spectra have been normalized to the low-frequency lines (50–100  $\text{cm}^{-1}$ ) of  $\text{N}_2$  that appear in the spectra since the incident laser beam is focused at the sample.

previously, this required a second scattering geometry schematically illustrated in Figure 1b. Using these two geometries it was possible to identify the symmetry species of the observed bands since the contribution of different polarizability components to bands of the same symmetry species results in a variation in intensity of the same bands in these two geometries. This then facilitates the assignment to a specific symmetry species.

In the laboratory frame of reference shown in Figure 1a, the incident laser propagates along the *X* direction while the scattered light is viewed along the *Z* axis. The incident light can be polarized either along *Y* or *Z*, while the analyzer can be placed parallel to either *Y* or *X*. The designation for each Raman spectrum is due to Damen et al.<sup>21</sup> and is used to label the spectra in Figure 2. The scattering notation is of the form *A(BC)D* where *A* and *D* are the propagation directions of the incident (*A*) and scattered (*D*) radiation while *B* and *C* refer to the direction of polarization of the incident (*B*) and analyzed (*C*) radiation, respectively. Thus in the top spectrum of Figure 2 the light is incident along the *X* direction with *Y* polarization while the scattered light is collected in the *Z* direction with the analyzer placed parallel to the *Y* axis.

As is shown in the spectra displayed in Figure 2, the anisotropic scattering properties of the filament are evident. This set of polarized Raman measurements was designed to select out modes belonging to each of the Raman-active symmetry species through knowledge of the chain orientation with respect to the filament axis, the factor group symmetry and the Raman-scattering activities. For the planar zigzag form of  $\text{PVF}_2$ , the factor group of the line group is isomorphic to the  $C_{2v}$  point group. The vibrations are distributed among the symmetry species as follows:  $5A_1 + 2A_2 + 3B_1 + 4B_2$  with all but the  $A_2$  (IR inactive) species being both IR and Raman active.

The unique symmetry axis ( $C_2$ ) of the planar backbone of  $\text{PVF}_2$  is perpendicular to the chain axis and therefore perpendicular to the orientation direction. Although this relationship between symmetry axis and orientation is different from those treated by Snyder,<sup>20</sup> recent work<sup>16</sup> has

**Table I**  
Raman Scattering Activities for Planar Zigzag Structure of  $\text{PVF}_2$  (Geometry A)

polarizn expt	symmetry species			
	$A_1$	$A_2$	$B_1$	$B_2$
$X(YY)Z$	$\alpha_{xx}$	0	0	0
$X(ZY)Z$	0	$\alpha_{xy}$	$\alpha_{xz}$	0
$X(YX)Z$	0	$\alpha_{xy}$	$\alpha_{xz}$	0
$X(ZX)Z$	$\alpha_{yy}, \alpha_{zz}$	0	0	$\alpha_{yz}$

**Table II**  
Contributions to the Raman Scattering Activities for Planar Zigzag Structure of  $\text{PVF}_2$  (Geometry B)

polarizn expt	symmetry species	
	$A_1$	$B_2$
$X(YY)Z$	$1/32(12\alpha_{yy}^2 + 24\alpha_{yy}\alpha_{zz} + 12\alpha_{zz}^2)$	$1/2\alpha_{yz}^2$
$X(ZY)Z$	$1/32(4\alpha_{yy}^2 - 8\alpha_{yy}\alpha_{zz} + 4\alpha_{zz}^2)$	$1/2\alpha_{yz}^2$

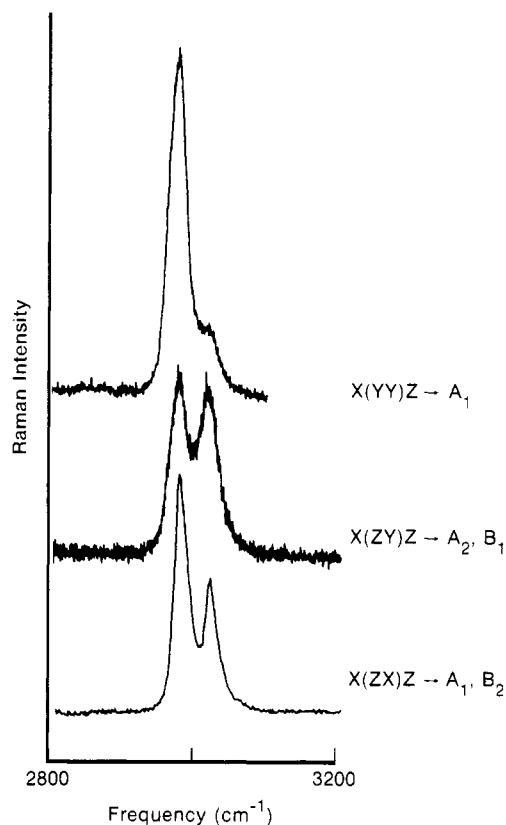


**Figure 3.** Polarized Raman spectra of  $\text{PVF}_2$  (form I) (geometry A) in the 2800–3200- $\text{cm}^{-1}$  region. As seen by the S/N ratio of the  $X(ZY)Z$  spectrum, it has been expanded by 4 times, and it is included for qualitative comparison only.

reported orientation averages for just such a case. In Table I the results for geometry A are summarized. Several important conclusions can be drawn from this table, which, when used in conjunction with the polarization measurements, allow the assignment of the observed bands to a particular symmetry species.

After examination of this table it becomes apparent that the  $X(YY)Z$  experiment selects out the totally symmetric symmetry species ( $A_1$ ) and, when it is taken in conjunction with the  $X(ZX)Z$  spectrum, it should allow assignment of the  $B_2$  bands since they will have been absent in the initial spectrum. The obvious differences between the  $X(YY)Z$  and  $X(ZX)Z$  spectra in Figures 2 and 3 (CH stretch region) suggest at least four bands that have  $A_1$  symmetry and three that can be assigned to the  $B_2$  symmetry species. Those at 2976, 1432, 1277, and 840  $\text{cm}^{-1}$  exhibit  $A_1$  symmetry, while those at 3020, 876, and 442  $\text{cm}^{-1}$  belong to the

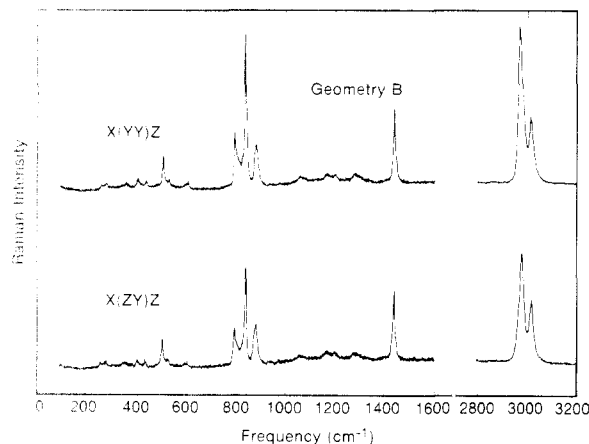


**Figure 4.** Polarized Raman measurements of PVF<sub>2</sub> (form I) in geometry B. Spectra have been normalized so that a direct comparison of intensities can be made.

$B_2$  symmetry species. It is, at first, tempting to assign the medium bands observed at 610 and 800 cm<sup>-1</sup> to the  $A_1$  species until one examines the polarization results with geometry B. In Table II are listed the polarizability contributions to the  $A_1$  and  $B_2$  symmetry species for two experiments in this alternative scattering geometry. Although the intensity of the band of  $B_2$  symmetry should remain constant in both measurements, the intensity of those belonging to the  $A_1$  species should be larger in the  $X(YY)Z$  spectrum. As observed in Figure 4, the previously assigned  $A_1$  bands increase in intensity, even if only slightly, in going from the  $X(ZY)Z$  to the  $X(YY)Z$  spectrum, while the  $B_2$  bands remain unchanged. In addition a band of medium intensity is observed at 510 cm<sup>-1</sup> that is assigned to the missing  $A_1$  mode. It is apparent from Figure 4 that the 610-cm<sup>-1</sup> band is absent, while the 800-cm<sup>-1</sup> band exhibits  $A_1$  behavior. As discussed in more detail in a later section, these bands are attributable to residual form II introduced in a small amount during drawing.

The assignment of the remaining  $B_2$  vibration from the observed Raman spectra is aided by polarized infrared results on oriented films that have appeared in the literature<sup>11</sup> and have been reproduced in this laboratory. The strongest IR band observed when the incident beam is polarized perpendicular to the orientation direction is found at 1185 cm<sup>-1</sup>. This corresponds to the broad new feature that is observed in the lower spectrum [ $X(ZX)Z$ ] of Figure 2 in which bands attributable to the  $B_2$  symmetry species should appear. Hence, tentatively the Raman band at 1170 cm<sup>-1</sup> is assigned to the remaining  $B_2$  vibration.

Identification of the  $B_1$  modes is straightforward, whereas the assignment of the  $A_2$  vibrations is more complex since the IR results can offer no assistance because the  $A_2$  bands are IR inactive. From the comparison of the  $X(YY)Z$  spectrum with that obtained in the  $X(ZY)Z$  polarization shown in Figure 2, it becomes apparent that there is residual intensity of the strong  $A_1$  modes in the latter, indicating that leakage occurs due to a lack of perfect orientation, the presence of noncrystalline material, and/or physical misalignment of the filament in the laser beam. The last possibility can, for the most part, be discounted by reference to Figure 5. As indicated in Table I the  $X(ZY)Z$  and  $X(YX)Z$  measurements should give identical spectra. The extent of deviation from equal intensities is indicative of sample misalignment in the beam which, as indicated in Figure 5, is minimal. In addition to the leakage of bands from other polarizations due to lack of perfect uniaxial orientation, a number of new

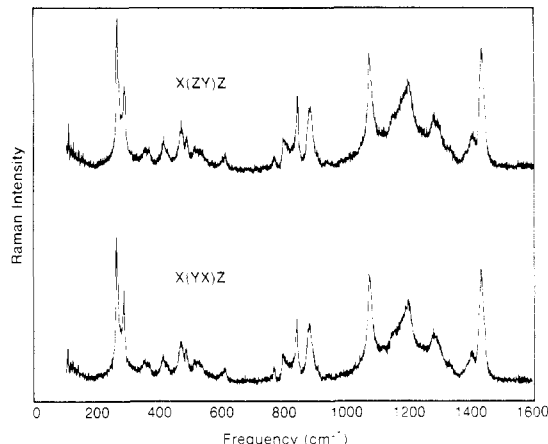


**Figure 5.** Polarized Raman spectra of form I using scattering geometry A. For an oriented filament perfectly aligned perpendicular to the incident laser, the  $X(ZY)Z$  and  $X(YX)Z$  spectral intensities would be identical. Any deviation is indicative of macroscopic misalignment. Spectra have been normalized to low-frequency N<sub>2</sub> lines.

**Table III**  
Symmetry Assignment of the Observed Bands

symmetry species	frequency, cm <sup>-1</sup>			assign <sup>a,b</sup>
	Raman	infrared <sup>a</sup>	calcd <sup>a</sup>	
$A_1$	2976	2982	2980	$\nu_s(\text{CH}_2)$
	1432	1432	1434	$\delta(\text{CH}_2)$
	1277 <sup>c</sup>	1278	1185	$\delta(\text{CCC}) + \nu_s(\text{CF}_2) + \nu_s(\text{CC})$
	840 <sup>c</sup>	842	886	$\nu_s(\text{CF}_2)$
	510	511	516	$\delta(\text{CF}_2)$
$A_2$	1200		991	t(CH <sub>2</sub> )
	263		270	t(CF <sub>2</sub> )
$B_1$	1400	1403	1398	w(CH <sub>2</sub> ) + $\nu_a(\text{CC})$
	1076	1074	1063	$\nu_a(\text{CC}) + \text{w}(\text{CH}_2) + \text{w}(\text{CF}_2)$
	467	470	484	w(CH <sub>2</sub> )
$B_2$	3020	3019	3020	$\nu_a(\text{CH}_2)$
	1170 <sup>c</sup>	1185	1257	$\nu_a(\text{CF}_2) + \text{r}(\text{CF}_2) + \text{r}(\text{CH}_2)$
	876 <sup>c</sup>	882	843	r(CH <sub>2</sub> ) + $\nu_a(\text{CF}_2)$
	442	448	483	r(CF <sub>2</sub> ) + $\tau(\text{CC}) + \text{r}(\text{CH}_2)$

<sup>a</sup> From ref 11. <sup>b</sup>  $\nu$ , stretch;  $\delta$ , bend; t, twist; r, rock; w, wag;  $\tau$ , torsion. <sup>c</sup> From ref 11 but mode assignment changed.

bands are observed that can be assigned to  $A_2$  and  $B_1$  symmetry species. In particular, the medium band at 1076 cm<sup>-1</sup>, whose IR counterpart is observed at 1074 cm<sup>-1</sup> and is parallel polarized, can be assigned to a  $B_1$  species. Similarly, the Raman bands observed at 467 and 1400 cm<sup>-1</sup> corresponding to the parallel IR bands at 470 and 1400 cm<sup>-1</sup> also exhibit  $B_1$  symmetry. On the other hand the medium-strong band found at 263 cm<sup>-1</sup> that has no IR counterpart can definitely be assigned to an  $A_2$  vibration. Of the remaining bands not attributable to residual form II, only those at 769 and 1200 cm<sup>-1</sup> are candidates for assignment to the  $A_2$  symmetry species. Since the Raman band at 769 cm<sup>-1</sup> corresponds to the IR band at 769 cm<sup>-1</sup> it cannot be an  $A_2$  vibration and could be due to the presence of head-to-head defects. This then suggests that the weak 1200-cm<sup>-1</sup> band that has no IR counterpart can be assigned to the  $A_2$  symmetry species.

The assignments of the polarized Raman bands are summarized in Table III, where they are compared with IR measurements<sup>11</sup> and normal coordinate calculations<sup>11</sup> that have appeared in the literature.

**Additional Band Assignments.** Not all of the observed bands in the polarized Raman spectra could be accounted for by assuming the presence of solely the planar zigzag conformation of PVF<sub>2</sub>. Additional bands could be introduced by the presence of different crystallographic forms and/or by chemical defects such as head-to-head

Table IV  
Assignment of Additional Bands Observed in Raman  
Spectra of Planar Zigzag PVF<sub>2</sub>

frequency, cm <sup>-1</sup>	assignment
1441	$\delta(\text{CH}_2)$ in $(\text{CH}_2\text{CH}_2)_n$ sequences
800	residual form II
769 <sup>a</sup>	$\nu(\text{CF}_2) + \nu(\text{CC})$ in $(\text{CF}_2\text{CF}_2)_n$ sequences
606	residual form II
482	residual form II
410	residual form II
283	residual form II
23	longitudinal acoustical mode (LAM)

<sup>a</sup> Observed in perfluorobutane.<sup>22</sup>

linkages known to exist in PVF<sub>2</sub>.

In studies of oriented form I produced by drawing films of form II, Cessac and Curro<sup>19</sup> found that the intensity of Raman bands at 805, 605, 410, and 285 cm<sup>-1</sup> increased relative to the other bands in the spectrum as a function of stretching temperature. Since stretching at elevated temperatures is known<sup>18</sup> to produce oriented form II, they assigned these bands to residual form II. Bands of weak to medium intensity were also found at these positions in our study and together with the band at 482 cm<sup>-1</sup> are attributed<sup>10</sup> to residual form II (detected previously in the WAXD study), most probably introduced during the processing stage. In addition, vibrational bands were also observed at 769 and 1441 cm<sup>-1</sup> that originate from the presence of head-to-head defects.

A summary of the bands observed in addition to those assignable to the vibrations of planar zigzag PVF<sub>2</sub> can be found in Table IV.

**Observation of a Longitudinal Acoustical Mode (LAM).** Observations of the Raman-active longitudinal acoustical mode (LAM) in perfluoropolymers and copolymers has become increasingly more prevalent.<sup>13,23,24</sup> In highly oriented transparent specimens, the identification of LAM is facilitated through polarization studies since it is a highly polarized vibration of a crystalline chain stem. In addition, through careful control of the thermal and mechanical processing history, transparent filaments can be produced that greatly reduce scattered stray light near the exciting line, thereby permitting studies in the very low-frequency (5–30 cm<sup>-1</sup>) region where LAM in semi-crystalline polymers is found.<sup>24</sup>

As shown in Figure 6, a highly polarized Raman band is observed at 23 cm<sup>-1</sup> in the X(YY)Z polarization but is totally absent in the X(YX)Z spectrum. This intensity behavior suggests that this vibration belongs to the totally symmetric symmetry species as would be expected for a planar zigzag structure undergoing accordionlike motion. As seen in the difference spectrum, the bandwidth is on the order of 20 cm<sup>-1</sup>, indicating a broad distribution of chain stems within a given crystal and/or a broad distribution of lamellae thicknesses in this sample. This is not unusual for polymers that have been extruded and drawn.<sup>25</sup> One ramification of such a large bandwidth is that the correction of the scattering intensity for both frequency and temperature will shift the peak frequency by 5–6 cm<sup>-1</sup> to higher wavenumbers as shown by Snyder and Scherer.<sup>26</sup> Thus the actual position of LAM in form I PVF<sub>2</sub> is 28–29 cm<sup>-1</sup> in the region expected for a planar zigzag structure.

SAXS measurements revealed a four-point pattern indicative of lamella tilt (by 26°) with respect to the filament axis. The observed long period was 103 Å, which corresponds to a projected length of 113 Å after chain tilt is taken into account. Depending on the extent of the fold surface and thus the crystallinity, the actual stem length would be between 58 and 91 Å. The corresponding LAM

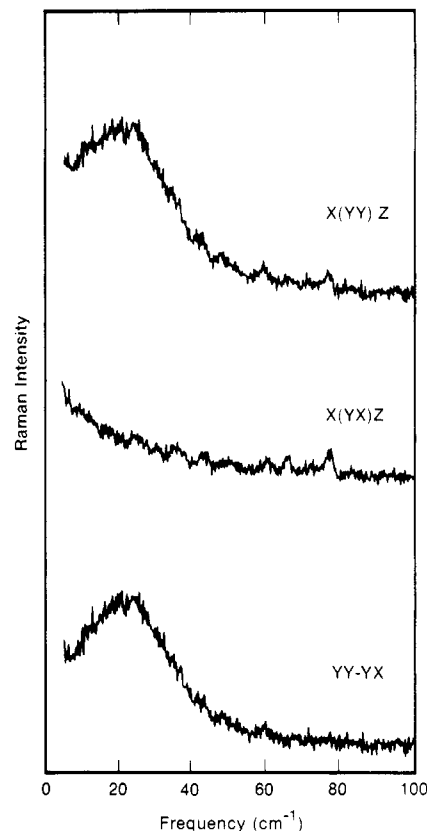


Figure 6. Low-frequency (10–100 cm<sup>-1</sup>) Raman spectra of form I obtained with a molecular I<sub>2</sub> filter to reduce stray light. Bottom spectrum represents the difference X(YY)Z – X(YX)Z.

frequency in polyethylene for stems of this length would be 35–45 cm<sup>-1</sup>, higher than that observed for planar zigzag PVF<sub>2</sub>. However, upon considering the uniform elastic rod model,<sup>24</sup> this undoubtedly reflects the increase in crystalline density due to the heavy fluorine atoms. When this is taken into account, the *c* axis Young's modulus, as obtained from the elastic-rod model,<sup>24</sup> of both PE and planar PVF<sub>2</sub> are similar, as would be expected in the absence of any freedom of rotation about bonds known to be responsible for a lowering of the axial modulus in helical structures.<sup>27</sup>

## Conclusion

Polarized Raman scattering measurements on uniaxially oriented PVF<sub>2</sub> (form I) have allowed the assignment of the observed bands to their respective symmetry species. The anisotropic scattering profiles of an oriented filament have been analyzed in two different scattering geometries and compared to existing IR data in order to ensure that all vibrational bands exhibit consistent polarization properties. Results indicate that previous band assignments must be revised, prompting also a reexamination of force fields previously used in normal mode calculations of planar zigzag PVF<sub>2</sub>.

An intense highly polarized Raman band was observed in the low-frequency region at 23 cm<sup>-1</sup>, and after an examination of its polarization properties it was assigned to the longitudinal acoustical mode (LAM). This is the first time that LAM has been observed in any of the crystalline modifications of PVF<sub>2</sub>, and it suggests that the LAM band may prove useful in understanding the structure and morphology responsible for the piezoelectric and ferroelectric properties that it exhibits.

**Acknowledgment.** We wish to thank Professor E. S. Clark (University of Tennessee) for the WAXD and SAXS

photographs and Dr. N. E. Schlotter (Bell Communications Research) for many helpful discussions.

**Registry No.** PVF<sub>2</sub> (homopolymer), 24937-79-9.

## References and Notes

- (1) Kepler, R. G.; Anderson, R. A. *CRC Crit. Rev. Solid State Mater. Sci.* **1980**, *9*, 399.
- (2) Lovinger, A. J. In "Developments in Crystalline Polymers 1"; Basset, D. C., Ed.; Applied Science: London, 1982.
- (3) Hasegawa, R.; Takahashi, Y.; Chatani, Y.; Tadokoro, H. *Polym. J. (Tokyo)* **1972**, *3*, 600.
- (4) Yagi, T.; Tatemoto, M.; Sako, J. *Polym. J. (Tokyo)* **1980**, *12*, 209.
- (5) Davis, G. T.; Furukawa, T.; Lovinger, A. J.; Broadhurst, M. G. *Macromolecules* **1982**, *15*, 329.
- (6) Koizumi, N.; Murata, Y.; Oka, Y. *Jpn. J. Appl. Phys.* **1984**, *23*, L324.
- (7) Enomoto, S.; Kawai, Y.; Sugita, M. *J. Polym. Sci., Polym. Phys. Ed.* **1968**, *6*, 861.
- (8) Cortili, G.; Zerbi, G. *Spectrochim. Acta, Part A* **1967**, *23A*, 285.
- (9) Rabolt, J. F.; Johnson, K. W. *J. Chem. Phys.* **1973**, *59*, 3710.
- (10) Kobayashi, M.; Tashiro, K.; Tadokoro, H. *Macromolecules* **1975**, *8*, 158.
- (11) Bachmann, M. A.; Koenig, J. L. *J. Chem. Phys.* **1981**, *74*, 5896.
- (12) Boerio, F. J.; Koenig, J. L. *J. Polym. Sci., Polym. Phys. Ed.* **1971**, *9*, 1517.
- (13) Zabel, K.; Schlotter, N. E.; Rabolt, J. F. *Macromolecules* **1983**, *16*, 446.
- (14) Wilson, F. C.; Starkweather, H. W., Jr. *J. Polym. Sci., Polym. Phys. Ed.* **1973**, *11*, 919.
- (15) Farmer, B.; Lando, J. B. *J. Macromol. Sci., Phys.* **1975**, *B11*, 89.
- (16) Schlotter, N. E.; Rabolt, J. F. *Polymer* **1984**, *25*, 165.
- (17) Devlin, G. E.; Davis, J. L.; Chase, L.; Geschwind, S. *Appl. Phys. Lett.* **1971**, *19*, 138.
- (18) McGrath, J. C.; Ward, I. M. *Polymer* **1980**, *21*, 855.
- (19) Cessac, G. L.; Curro, J. G. *J. Polym. Sci., Polym. Phys. Ed.* **1974**, *12*, 695.
- (20) Snyder, R. G. *J. Mol. Spectrosc.* **1971**, *37*, 353.
- (21) Damen, T. C.; Porto, S. P. S.; Tell, B. *Phys. Rev.* **1966**, *142*, 570.
- (22) Campos-Vallette, M.; Rey-Lafon, M.; Lagmier, R. *Chem. Phys. Lett.* **1982**, *89*, 189.
- (23) Rabolt, J. F. *Polymer* **1981**, *22*, 890.
- (24) Rabolt, J. F. *CRC Rev. Solid State Mater. Sci.* **1985**, *12*, 165.
- (25) Wang, Y. K.; Waldman, D. A.; Lasch, J. E.; Stein, R. S.; Hsu, S. L. *Macromolecules* **1982**, *15*, 1452.
- (26) Snyder, R. G.; Scherer, J. R. *J. Polym. Sci., Polym. Phys. Ed.* **1980**, *18*, 421.
- (27) Fanconi, B.; Rabolt, J. F. *J. Polym. Sci., Polym. Phys. Ed.* **1985**, *23*, 1201.

## Orientation of Poly(octadecyl methacrylate) and Poly(octadecyl acrylate) in Langmuir-Blodgett Monolayers Investigated by Polarized Infrared Spectroscopy

Stephen J. Mumby,\*† J. D. Swalen, and J. F. Rabolt

IBM Almaden Research Center, San Jose, California 95120-6099.

Received November 26, 1985

**ABSTRACT:** Molecular orientation in Langmuir-Blodgett (L-B) monolayers of poly(octadecyl methacrylate) (PODMA) and poly(octadecyl acrylate) (PODA) has been studied by infrared spectroscopy. Substantial anisotropy between the spectra measured in transmission, and by reflection at grazing incidence, was observed for both these polymers. The carbonyl group was found to be oriented approximately perpendicular to the substrate surface, independent of polymer type and of deposition surface pressure within the range investigated. The long aliphatic ester side groups were also found to be approximately perpendicular to the plane of the monolayer. However, the orientation of these groups was strongly dependent upon the chemical structure of the polymer used and on the surface pressure at transfer. More condensed L-B monolayers of PODA could be formed than was the case for PODMA, in part due to the lower steric hindrance to rotations about backbone bonds in PODA because of the absence of the methyl side group.

## Introduction

The Langmuir-Blodgett (L-B) technique for the deposition of ordered monolayers of amphiphilic molecules on solid substrates has obtained new prominence since the incorporation of L-B films into microelectronic devices. This renaissance has also been inspired by the wide range of other potential technological applications of L-B films<sup>1-3</sup> and by the opportunities to investigate the structure and properties of the molecules in this uniquely ordered environment. However, from the technological standpoint, L-B films of traditionally used amphiphilic materials, such as long-chain fatty acids, are rather fragile, possessing little mechanical or thermal stability or resistance to dissolution. Consequently, efforts have been made to extend the range of materials that may be transferred as monolayers by the

L-B technique.<sup>4</sup> Cemel et al<sup>5</sup> first suggested the polymerization of monolayers or multilayers of unsaturated molecules to produce a more robust structure while still retaining the orientation of the monomers. This technique has met with some success; related polymerized liposome structures have been investigated as potential drug carriers<sup>6</sup> and as useful models for cell membranes.<sup>7</sup> However, recent studies<sup>8,9</sup> have revealed that internal stresses, which are frequently generated by polymerization after transfer of the monomer to a substrate, can produce films with large fissures and cracks. One possible means of eliminating this stress is to polymerize a mixture of isomers such that the average area per monomer unit is unchanged after polymerization. This strategy has been adopted by Rabe et al<sup>10</sup> using the two isomers: octadecylfumaric acid and octadecylmaleic acid. In an alternative approach, efforts have been directed toward transferring L-B monolayers of preformed polymers that do not exhibit these inherent stress problems. Structure-property relationships may also

\* Present address: AT&T Bell Laboratories, Room 7C-050, Whippany Road, Whippany, NJ 07981.